

Quantum Mechanical Study of the Potential Energy Surface of the ClO + NO₂ ReactionSaša Kovačič,[†] Antonija Lesar,^{*,†} and Milan Hodošček^{†,‡}Department of Physical and Organic Chemistry, Institute Jožef Stefan, Jamova 39,
SI-1000 Ljubljana, Slovenia, and Centre for Molecular Modeling, National Institute of Chemistry,
Hajdrihova 19, SI-1000 Ljubljana, Slovenia

Received June 24, 2004

In the study of the reaction pathways of the ClO + NO₂ reaction including reliable structures of the reactants, products, intermediates, and transition states as well as energies the MP2/6-311G(d), B3LYP/6-311G(d), and G2(MP2) methods have been employed. Chlorine nitrate, ClONO₂, is formed by N–O association without an entrance barrier and is stabilized by 29.8 kcal mol^{−1}. It can undergo either a direct 1,3 migration of Cl or OCl rotation to yield an indistinguishable isomer. The corresponding barriers are 45.8 and 7.1 kcal mol^{−1}, respectively. ClONO₂ can further decompose into NO₃ + Cl with an endothermicity of 46.4 kcal mol^{−1}. The overall endothermicity of the NO₂ + ClO → NO₃ + Cl reaction is calculated to be 16.6 kcal mol^{−1}. The formation of cis-perp and trans-perp conformer of chlorine peroxyxynitrite, ClOONO_{ep} and ClOONO_{tp}, are exothermic by 5.4 and 3.8 kcal mol^{−1}, respectively. Calculations on the possible reaction pathways for the isomerization of ClOONO to ClONO₂ showed that the activation barriers are too high to account for appreciable nitrate formation from peroxyxynitrite isomerization. All quoted relative energies are related to G2(MP2) calculations.

I. INTRODUCTION

Chlorine nitrate, ClONO₂, was first recognized as an important temporary reservoir for reactive chlorine and NO_x by Rowland et al.^{1,2} It is formed primarily through the recombination reaction of the ClO radicals and NO₂



and is consequently responsible for a significant reduction of efficiency with which chlorine destroys ozone in the stratosphere. The rates of formation and photodissociation of ClONO₂ greatly influence the atmospheric concentration of ClO. Several photochemical channels that involve single bond fission are



Initial studies have reported that the dissociative channels (2) and (3) are dominant.^{3,4} The first direct observation of the ClO product channel was performed by Minton et al.⁵ The branching ratios for various dissociation pathways, their wavelength, and their pressure dependence have been widely investigated. Recent studies of the photochemistry of ClONO₂ are summarized in the NASA Panel for Data Evaluation.⁶

Numerous experimental investigations using various technique have been carried out to determine the rate constant of the ClO + NO₂ association reaction. The results are in good agreement with one another; the reaction was found

to be pressure dependent and has a negative temperature dependence.⁷ Molina et al.⁸ have reported an indication that a species other than ClONO₂ are likely to be formed; among them, the chlorine peroxyxynitrite isomer, ClOONO, would be the preferred one. Further evidence for the existence of ClOONO have been provided by matrix isolated IR spectra.⁹ Subsequent investigations of the identity of the products formed in the ClO + NO₂ reaction have shown that ClONO₂ is the only product¹⁰ and ruled out the possible existence of any other isomer.

The calculations performed by McGrath¹¹ have revealed that ClOONO formation is thermodynamically disfavored above 220 K. Other theoretical studies related to this reaction are mainly limited to the structure and vibrational frequencies of chlorine nitrate and chlorine peroxyxynitrite.^{12–15} Calculations on excited electronic states of ClONO₂ have been provided by Grana.¹⁶

The present ab initio calculations using three levels of theory are intended to study the possible pathways for the ClO + NO₂ reaction including reliable structures of the reactants, products, intermediates, and transition states as well as their relative energies. Thus, we have considered the formation of the ClONO₂ and ClOONO isomers and their isomerization reaction, ClOONO ↔ ClONO₂. The computational methods employed in these investigations are described in the next section, followed by the presentation and discussion of results. The main conclusions are summarized in the final section.

II. COMPUTATIONAL METHODS

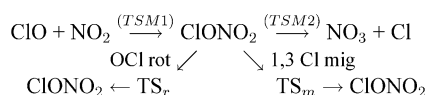
The electronic molecular orbital calculations were carried out using the GAUSSIAN 98 program.¹⁷ Geometries of reactants, adducts, and transition state structures were fully optimized with the second-order Moller–Plesset (MP2)

* Corresponding author e-mail: antonija.lesar@ijs.si.

[†] Institute Jožef Stefan.

[‡] National Institute of Chemistry.

Scheme 1



method¹⁸ and the Becke three-parameter nonlocal exchange functional¹⁹ with the nonlocal correlation of Lee, Yang, and Parr (B3LYP).^{20,21} The standard triple ζ plus polarization 6-311G(d) basis set, as implemented in the program,¹⁷ was employed in the calculations. The harmonic frequencies of all species were computed from analytical derivatives at the MP2 and B3LYP levels using geometries calculated at these levels of theory in order to characterize the stationary points as either minima or first-order saddle points, to determine zero-point vibrational energies (ZPE), and to generate force constant data needed in the IRC calculations. The intrinsic reaction coordinate (IRC) method²² has been performed to track minimum-energy paths from the transition state structures to the corresponding minimum. A step size of 0.1 amu^{1/2} bohr was used in the IRC procedure. For the stationary points, we have also carried out the G2(MP2)²³ calculations to improve the energetics of reaction pathways.

III. RESULTS AND DISCUSSION

For the reaction of CIO radical with NO₂ we have considered two different main reaction channels resulting in the CIONO₂ and CIOONO formation. The formation of either adduct depends on the directions of mutual interaction of the reactants. CIONO₂ is formed when the oxygen atom of CIO is approaching to the nitrogen atom of NO₂, i.e., the O to N approach. If the oxygen atom attacks one of the oxygen atoms of NO₂, i.e., O to O approach, then CIOONO is formed. Further, the isomerization of CIOONO to CIONO₂, what is actually a nitrite-nitro rearrangement, has been examined.

The optimized geometrical parameters of the adducts and the transition states involved in the above processes at the MP2/6-311G(d) and B3LYP/6-311G(d) levels are displayed in Figures 1–3. The calculated unscaled harmonic vibrational frequencies of the stationary points at the B3LYP/6-311G(d) level are presented in Table 1. The corresponding zero-point corrected relative energies with regard to reactants at different levels of theory are given in Table 2. Figure 4 graphically summarizes the overall profile of the singlet potential energy surface at the G2(MP2) level of theory.

Three transition state structures were determined only at the MP2/6-311G(d) level of calculations and are denoted as TSM1, TSM2, and TSM3. On the other hand, the transition state structure denoted as TSB7 was only determined at the B3LYP/6-311G(d) level as it will be described in detail below. G2(MP2) energies for TSM2, TSM3, TS5, and TSB7 structures were not evaluated because the QCISD(T)/6-311G-(d,p) calculations in the G2(MP2) scheme were not converged. Hence, there are no entries in these cases in Table 2. Other structures resulted from MP2 and B3LYP levels of theory were found to be consistent as can be seen from Figures 1–3. Thus, the discussion in the following subsections is mainly related to the MP2 results, and only marked differences resulting from B3LYP calculations are pointed out.

(A) CIONO₂ Formation. The schematic representation of this process is given by Scheme 1. The optimized

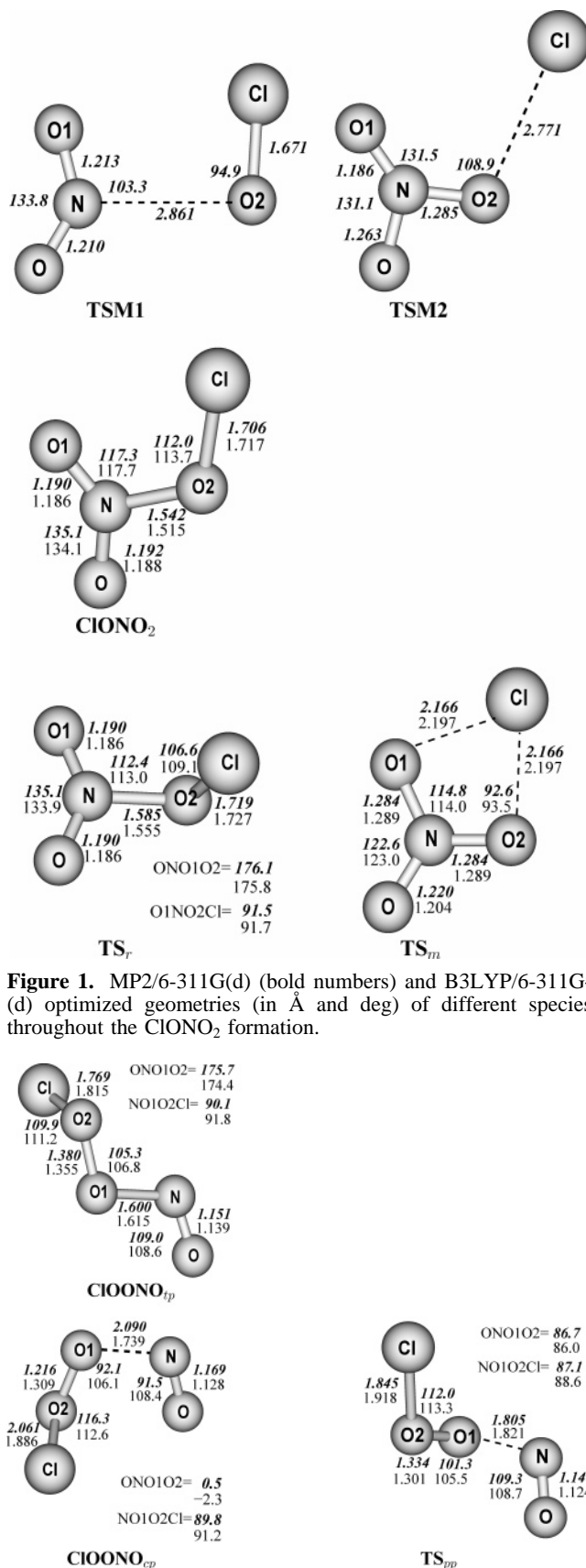


Figure 1. MP2/6-311G(d) (bold numbers) and B3LYP/6-311G(d) optimized geometries (in Å and deg) of different species throughout the CIONO₂ formation.

Figure 2. MP2/6-311G(d) (bold numbers) and B3LYP/6-311G(d) optimized geometries (in Å and deg) of different species throughout the CIOONO formation.

structures for the stationary points including the geometrical parameters are presented in Figure 1.

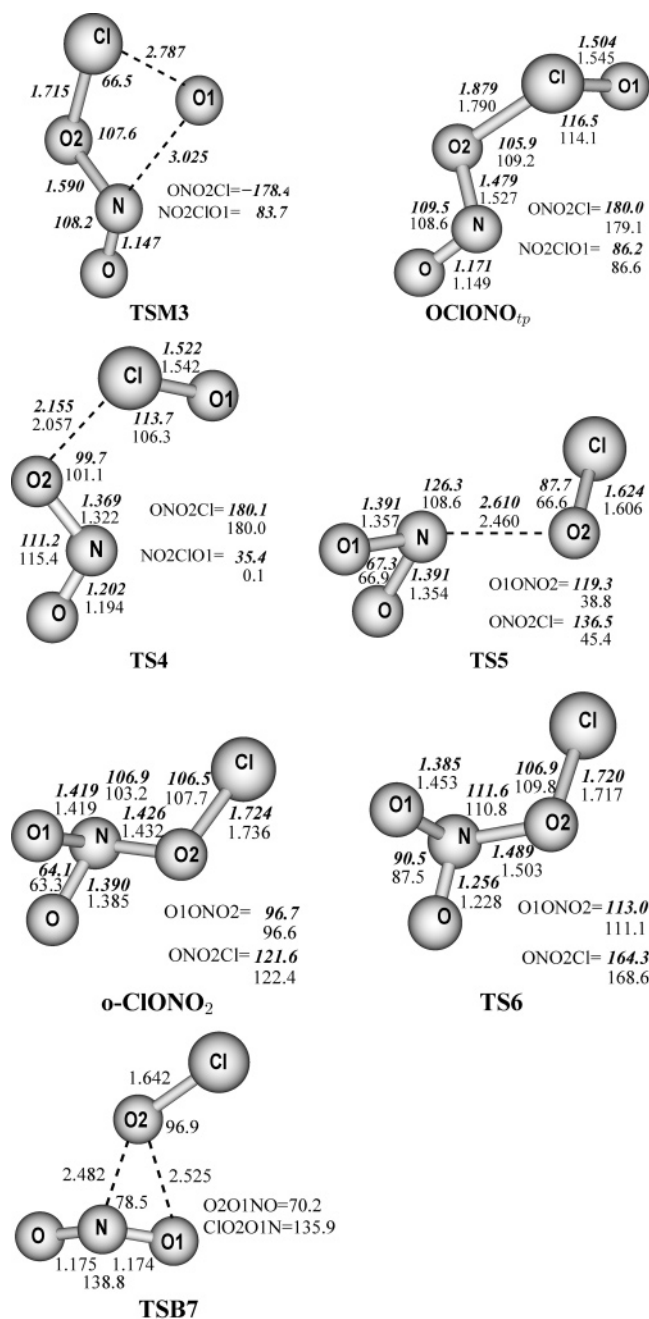


Figure 3. MP2/6-311G(d) (bold numbers) and B3LYP/6-311G(d) optimized geometries (in Å and deg) of different species throughout the $\text{ClONO}_2 \leftrightarrow \text{ClONO}_2$ isomerization.

In the course of the approach of the two radicals, the ClONO_2 adduct, known as chlorine nitrate, is formed without an entrance barrier. Nevertheless, the first-order saddle point, TSM1, was characterized in this region. The TSM1 structure exhibits a relatively early character: the ONO1 group almost kept the structure of the NO_2 molecule and the bond forming distance between N and O2 is 2.861 Å, while the ClO2N angle amounts to 94.9°. The MP2 imaginary frequency of 174i cm^{-1} is associated with N–O stretch normal mode. The calculated energy of the saddle point is 14.3 kcal mol^{-1} lower with respect to the reactants as can be seen from Table 2. The minimum energy structure of ClONO_2 has planar C_s symmetry and is stabilized by 36.4 kcal mol^{-1} . At the B3LYP level, the ClONO_2 formation is exothermic by 24.7 kcal mol^{-1} , thus it is 11.7 kcal mol^{-1} less stable than at the MP2

Table 1: Unscaled B3LYP/6-311G(d) Harmonic Vibrational Frequencies (cm^{-1}) of the Stationary Points in the $\text{ClO} + \text{NO}_2$ Reaction

	(a) Stable Species				
	ClONO_2	ClOONO_{tp}	ClOONO_{cp}	OCIONO_{tp}	o- ClONO_2
ν_1	130 (120) ^a	96	107	102	58
ν_2	244 (270)	176	193	168	276
ν_3	436 (434)	253	221	217	428
ν_4	558 (560)	329	308	306	479
ν_5	725 (711)	434	433	407	685
ν_6	774 (780)	563	571	433	734
ν_7	825 (809)	743	753	845	800
ν_8	1351 (1292)	995	1021	917	895
ν_9	1824 (1735)	1917	1973	1857	1203

	(b) Transition States					
	TS_r	TS_m	TS4	TS5	TS6	TSB7
ν_1	105i	793i	515i	157i	1031i	534i
ν_2	209	152	123	81	77	71
ν_3	483	378	176	189	190	113
ν_4	508	610	225	248	385	155
ν_5	665	759	370	496	469	252
ν_6	814	766	643	638	626	651
ν_7	818	936	765	791	731	775
ν_8	1358	1037	942	840	822	1336
ν_9	1824	1562	1626	1275	1289	1887

^a Fundamental vibrational frequencies from ref 24.

Table 2: Zero-Point Corrected Relative Energies, ΔE_0 (kcal mol^{-1})

species	ΔE_0		
	MP2 ^a	B3LYP ^b	G2(MP2) ^c
$\text{NO}_2 + \text{OCl}$	0.0	0.0	0.0
$\text{NO}_3 + \text{Cl}$	−6.7	4.7	16.6
TSM1	−14.3		−3.2
ClONO_2	−36.4	−24.7	−29.8
TSM2	6.2		
TS_r	−29.4	−17.0	−22.7
TS_m	15.3	20.9	16.0
ClOONO_{tp}	−2.7	1.8	−3.8
TS_{pp}	3.7	8.1	4.7
ClOONO_{cp}	−8.2	−0.6	−5.4
TSM3	99.5		
OCIONO_{tp}	22.3	28.8	5.6
TS4	24.2	36.0	15.1
TS5	78.6	104.1	
o- ClONO_2	47.3	55.9	42.1
TS6	79.9	80.8	68.6
TSB7		27.4	

^a TSB7 structure was not able to be determined at the MP2/6-311G(d) level. ^b All attempts to locate TSM1, TSM2, and TSM3 structures at the B3LYP/6-311G(d) level were proved futile. ^c QCISD(T)/6-311G(d,p) calculations in the G2(MP2) scheme were not converged for the TSM2, TSM3, TS5, and TSB7.

level. The obtained equilibrium structure is in reasonable agreement with the experimental gas-phase data²⁵ and CCSD-(T)/TZ2P molecular geometry.¹⁵ From ClONO_2 the reaction can proceed to the $\text{NO}_3 + \text{Cl}$ radicals production. Also in the process of decomposition of chlorine nitrate the first-order saddle point, TSM2, is identified. The Cl–O2 bond length in TSM2 is elongated to 2.771 Å, and the central N–O2 bond (1.285 Å) becomes stronger. The reaction coordinate is associated with a frequency of 324i cm^{-1} . The calculated MP2 energy places TSM2 42.6 kcal mol^{-1} higher than ClONO_2 , and the endothermicity of the $\text{ClONO}_2 \rightarrow \text{NO}_3 + \text{Cl}$ reaction step is 29.7 kcal mol^{-1} . ClONO_2 can undergo two internal conversions. First, a 1,3 migration of Cl occurs

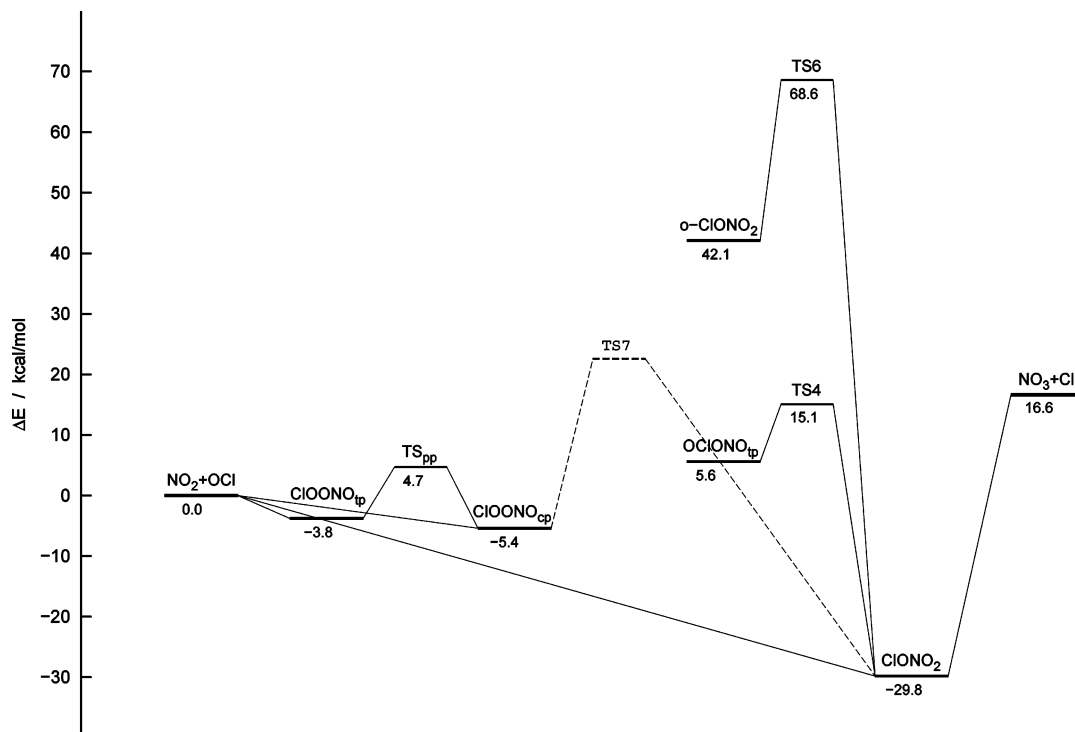
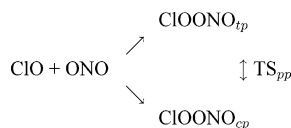


Figure 4. The overall profile of the potential energy surface for the CIO + NO₂ reaction calculated at the G2(MP2) level of theory. For TSB7, 23 kcal mol⁻¹ is estimated value (see text).

Scheme 2



through a planar four-center transition state TS_m and leads to an indistinguishable isomer. The O2...Cl bond in the TS_m has elongated from 1.706 in CIONO₂ to 2.166 Å in the transition state structure. The barrier for the internal migration is 51.7 kcal mol⁻¹ at the MP2 level of theory. Second, the O2–Cl rotation around the N–O2 bond is accompanied by an energy barrier of 7.0 kcal mol⁻¹. In going from CIONO₂ to the transition state for rotation, TS_r, insignificant structural changes exist, except for the ClO2NO1 torsional angle. TS_r structure has nearly a perpendicular arrangement of ClO2NO1 and O2NO1O torsional angles. The barriers for the Cl migration and OCl rotation in CIONO₂ are 5.9 kcal mol⁻¹ lower and 0.7 kcal mol⁻¹ higher, respectively, at the B3LYP level than those calculated at the MP2 level of theory.

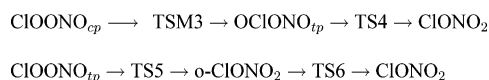
(B) CIOONO Formation. The formation of CIOONO takes place from the association of CIO with NO₂ from the oxygen side. The CIOONO isomer possesses two stable forms, cis-perp and trans-perp, differing in their conformation with respect to the O2–O1 and N–O1 bonds in accordance with previous investigations.¹¹ The schematic view of the reaction channels is given in Scheme 2, while the optimized structures for both CIOONO conformers and transition state are depicted in Figure 2.

When a comparison is made between NO₂ radical and CIOONO_{tp}, we can see a shrinkage of the N–O bond to 1.151 Å and an elongation of the N–O1 bond to 1.600 Å in CIOONO_{tp}; the bond angle is distinctly compressed to 109°. Also, the O2–Cl bond (1.769 Å) is elongated compared to its value in the OCl radical, calculated as 1.6075 Å at the

same level of theory. The NO1O2 and O1O2Cl bond angles are predicted to be 105° and 110°, respectively. The geometrical parameters are in reasonable agreement with those reported by McGrath¹¹ at the MP2 level of theory. As we can see from Table 2, the CIOONO_{tp} formation is exothermic by 2.7 kcal mol⁻¹ relative to OCl+NO₂ at the MP2 level of theory, but the B3LYP calculations predict the endothermicity of 1.8 kcal mol⁻¹.

CIOONO_{tp} can easily transform to a cis-perp conformer, CIOONO_{cp}, which lies 5.5 kcal mol⁻¹ below the trans-perp form. The transition state TS_{pp} accompanying this interconversion has a perp-perp conformation, and the calculated energy barrier is 6.4 kcal mol⁻¹. At the MP2 level of calculations the bond lengths of the cis-perp conformer are changed by 0.3 Å in average, which is related to the trans-perp conformer. Clearly, the main difference is related to the ONO1O2 torsional angle being 0.5° for the former conformer. Inspection of geometrical parameters in Figure 2 reveals that the deviation between the MP2 and B3LYP values is markedly just for the cis-perp conformer of CIOONO. The deviation of the N–O1 and O2–Cl bond lengths between two methods is 0.35 and 0.17 Å, respectively, and is about 15° for the ONO1 and NO1O2 angles. Certainly, B3LYP/6-311G(d) parameters of this conformer are in better agreement with those from the MP2/6-31G(d) calculations reported by McGrath et al.,¹¹ which is also the case for BrOONO analogues.²⁶ As well, the geometry of CIOONO_{cp} at the CCSD(T)/6-311G(d) level of theory predicted in our previous paper²⁷ is in line with B3LYP/6-311G(d) results. Such unusual trends in the predicted bond lengths and valence bond angles for cis-perp conformer were found also in the MP2/6-311+G(d) study of alkaline peroxy nitrates,²⁸ and likely arise from the instability of the Hartree–Fock wave functions as a reference. This indicates that cis-perp geometry of peroxy nitrates is not adequately

Scheme 3



described at the MP2 method, especially in conjunction with higher quality of basis set.

(C) ClOONO \leftrightarrow ClONO₂ Isomerization. The most straightforward way for unimolecular isomerization would be the transfer of the OCl group from oxygen (O1) in ClO2O1NO to nitrogen to form ClONO₂, but at the MP2/6-311G(d) level of theory we were unable to generate the transition state structure for such nitrite-nitro rearrangement. On the other hand, we have characterized two different subchannels. Scheme 3 summarizes the steps involved in these isomerization pathways, and Figure 3 shows the equilibrium and transition state structures.

ClOONO_{cp} can undergo a conversion yielding OCIONO_{tp} via transition state TSM3. TSM3 is a loose transition state with the O1 atom 3.025 and 2.787 Å away from the N and Cl atoms, respectively. The ClO2NO group of TSM3 closely resembles the structure of chlorine nitrite. OCIONO_{tp} can be described as a third isomer of chlorine nitrate. Such an isomer has been proposed long ago by Molina,⁸ but any evidence of its presence has never been confirmed. The minimum energy structure for OCIONO_{tp} is a nonplanar with an O1ClO2N dihedral angle of 86.2°. The ONO2 angle is predicted to be 109.5° and is similar to that of the ClOONO_{tp} isomer (109.0°). Furthermore, a comparison of the O–N and N–O2 bond lengths of OCIONO_{tp} (1.171 and 1.479 Å, respectively) with those in ClOONO_{tp} (1.151 and 1.600 Å, respectively) reveals that the bonding in the NO₂ group between the two isomers is similar. However, the OCIONO isomer is a hypervalent Cl structure in contrast to ClOONO and ClONO₂, which are normal-valent structures. The bond distances of the internal and external Cl–O bonds are 1.879 and 1.504 Å, respectively. It is interesting to compare these values with the related bonds in the HOOCIO in which the valency of Cl atom is the same. The bond lengths of 1.874 and 1.511 Å, respectively, were predicted from the MP2/6-31G(d) calculations.^{29,30} Thus, the bonding is remarkably similar. When we compare the corresponding relative energies from Table 2, we can see that the MP2 energy barrier for ClOONO_{cp} \rightarrow OCIONO_{tp} isomerization is as high as 107.7 kcal mol^{−1}, and the OCIONO_{tp} is destabilized by 30.5 kcal mol^{−1} relative to ClOONO_{cp}. OCIONO_{tp} can further transform to chlorine nitrate, i.e., ClONO₂. This transformation involves transition state TS4 with an energy of only 1.9 and 7.2 kcal mol^{−1} higher relative to OCIONO_{tp} at B3LYP and MP2 methods, respectively, which makes the eventual OCIONO \rightarrow ClONO₂ interconversion possible. When a comparison is made of TS4 to the structure of OCIONO_{tp}, there are observable changes in the N–O2 and O2–Cl bond lengths and the ClO2N bond angle between two structures. The two bonds are about 0.1 Å shorter and 0.3 Å longer, respectively, while the bond angle is compressed by 6°. One can see that reverse ClONO₂ \rightarrow OCIONO isomerization is also unlikely, as the height of the energy barrier is 60.6 kcal mol^{−1}.

ClOONO_{tp} can isomerize to ClONO₂ in a two-step process. The 1,2 migration of the OCl group from O1 toward the N atom in the ClOONO structure leads to a o-ClONO₂. The

migration proceeds via the transition state TS5, and the energy barrier was found to be very high, 81.3 kcal mol^{−1}. The ONO1 bond angle in TS5 is significantly compressed (67.3°) compared to either the ClOONO_{tp} (109.0°) or ClONO₂ (135.1°) structure. The two N–O bonds of TS5 become equivalent (1.391 Å), the oxygen of OCl is displaced away from the migrating origin (O1), and the migrating terminus (N) by 3.612 and 2.610 Å, respectively. The ClO2NO and O2NOO1 dihedral angles are 136.5 and 119.3°, respectively. The magnitude of the imaginary frequency is 181i cm^{−1}. The marked difference between TS5 and o-ClONO₂ is related to the shortening of the N–O2 bond by 1.18 Å. o-ClONO₂ undergoes subsequent conversion leading to the stable ClONO₂ adduct. TS6 has been determined in the investigation of this step, which requires an activation energy of 32.6 kcal mol^{−1}. Considering the structural parameters, we can see the shrinking of the N–O and N–O1 bonds from o-ClONO₂ through TS6 to ClONO₂, 1.390 \rightarrow 1.256 \rightarrow 1.192 Å and 1.419 \rightarrow 1.385 \rightarrow 1.190 Å, respectively. The corresponding elongation of the N–O2 bond is 1.426 \rightarrow 1.489 \rightarrow 1.542 Å, respectively. The ONO1 bond angle is increasing, 64.1 \rightarrow 90.5 \rightarrow 135.1°, respectively. As shown by the calculations presented above it is very unlikely that the ClOONO would isomerize to ClONO₂ due to the presence of large energy barriers in both possible isomerization pathways considered above. Both pathways are two-step processes, and the first one could be considered as ClOONO \leftrightarrow OCIONO \leftrightarrow ClONO₂ isomerization.

However, B3LYP/6-311G(d) calculations also supported unimolecular isomerization of chlorine peroxyxynitrite to chlorine nitrate. Structural data of the nonplanar transition state structure, TSB7, which is formed as a result of OCl migration initiating from the ClOONO_{cp}, is also shown in Figure 3. When IRC analysis is used to verify the transition state, it goes to the correct reactant and product structures. Due to this process, two main structural differences exist between transition state TSB7 and stable ClOONO_{cp} isomer. First, the O1–O2 bond increases from 1.309 Å in ClOONO_{cp} to 2.525 Å in the transition state, while the N–O1 bond decreases from 1.739 to 1.174 Å, respectively. Second, ClOONO_{cp} has a nearly perpendicular arrangement of ClO2O1N and O2O1NO torsional angles, while their arrangement in TSB7 is reduced to about 66°. In the resulting transition state structure the bond distances from the oxygen atom of the OCl group to each atom of NO₂ moiety become nearly the same, namely 2.525 and 2.673 Å to either of the O atoms and 2.482 Å to the N atom. Thus, the transition state resembles an OCl weakly coupled to NO₂, and the isomerization can be considered as a dissociative-associative process. ClONO₂ is calculated to have 24.1 kcal mol^{−1} lower energy than ClOONO_{cp} so the isomerization is very exothermic, but the activation energy barrier of 28.0 kcal mol^{−1} is too high to account for appreciable nitrate formation from peroxyxynitrite unimolecular isomerization.

It is of interest to compare the properties of the transition state for ClONO₂ \rightarrow ClOONO unimolecular isomerization process with those of related investigations. Sumathy and Peyerimhoff³¹ reported the transition state for the isomerization of HOONO to HONO₂. Their value for the isomerization energy barrier at the B3LYP/6-311++G(d,p) level is 39.0 kcal mol^{−1}, and the structure is very similar to the structure of the chlorine analogue calculated here. The O–O

distance of 2.547 Å between OH and NO₂ fragments in a loose nonplanar transition structure was obtained. Just recently, the B3LYP/6-311++G(d,p) study of Lohr et al.³² on reaction of alkyl (R = CH₃, C₂H₅, C₃H₇, C₅H₁₁) peroxy radical with NO also involves ROONO isomerization to RONO₂. The investigation revealed that the transition states are characterized by nearly constant bond distances from oxygen of the RO group to NO₂ (2.53 to 2.59 Å) and the energy barriers for isomerization (33.7 ± 0.5 kcal mol⁻¹). Further, they reported that the imaginary frequencies of related transition states decrease in magnitude with increasing mass of the R group. The imaginary frequency (534i cm⁻¹) for chlorine TS calculated here is consistent with this finding. Thus, the comparison of chlorine, hydrogen, and alkyl analogues clearly shows that the transition state structures for nitrite-nitrate isomerization are very similar.

Relative Energetics from G2(MP2) Calculations. Figure 4 graphically summarizes the relative energetic pathways for the CIO + NO₂ reaction resulting from the G2(MP2) calculations. The G2(MP2) method has been shown to yield the average absolute deviation from experiment of 1.58 kcal mol⁻¹ for a large set of species containing first- and second-row elements.²³ It performed also well in predicting transition state properties.³³

At first, we like to mention the most important difference related to the MP2 and B3LYP energy calculations. The overall NO₂ + CIO → NO₃ + Cl reaction is endothermic by 16.6 kcal mol⁻¹, which is in reasonable agreement with the experimental value of 14.7 kcal mol⁻¹ evaluated from experimental heats of formation for NO₂, CIO, NO₃, and Cl from ref 6. We have seen that the B3LYP/6-311G(d) method underestimates the reaction energy by about 12 kcal mol⁻¹ and that the MP2/6-311G(d) method predicts even an exothermic reaction. This is not surprising since it is known that MP2 methodologies usually produce wrong energetic ordering for species of high spin multiplicity, such as doublet radicals.

At the G2(MP2) level of calculations, the CIONO₂ formation from NO₂ and CIO radicals is exothermic by 29.8 kcal mol⁻¹. This value is in a reasonable agreement with 26.8 kcal mol⁻¹ estimated from experimental enthalpies of formation⁶ $\Delta H_{f,0}^\circ$ for NO₂ of 8.6 kcal mol⁻¹ and for CIO of 24.2 kcal mol⁻¹, while calculated²⁷ $\Delta H_{f,0}^\circ$ for CIONO₂ of 7.0 kcal mol⁻¹ was used. The energy barrier for the OCl rotation in CIONO₂ is 7.1 kcal mol⁻¹, while that for Cl migration is 45.8 kcal mol⁻¹.

The CIOONO formation is slightly exothermic, and the reaction energies are -3.8 and 5.4 kcal mol⁻¹ for trans-perp and cis-perp conformers, respectively. The CIOONO_{ip} → CIOONO_{cp} isomerization occurs by overcoming a 8.5 kcal mol⁻¹ energy barrier. Further, the OCIONO_{ip} isomer is less stable by 9.4 kcal mol⁻¹ relative to the CIOONO_{ip}. The energy barrier for OCIONO_{ip} → CIONO₂ isomerization is small, 9.5 kcal mol⁻¹, thus this process would occur readily. The lack of MP2 geometry for the TSB7 geometry does not allow consideration of the G2(MP2) activation energy for the CIOONO ↔ CIONO₂ isomerization; however, it is estimated to be about 23 kcal mol⁻¹ if we speculate that the difference between G2(MP2) and B3LYP values for TSB7 is similar to those for CIOONO_{cp} and CIONO₂ being 4.8 and 5.1 kcal mol⁻¹, respectively.

IV. SUMMARY

Ab initio molecular orbital calculations have been employed to provide a fairly complete study of two possible pathways in the NO₂ + OCl reaction. From the results based mainly on the G2(MP2) calculations, the following conclusions can be drawn.

Depending on the direction of the two approaching radicals, either CIONO₂ or CIOONO can be formed. CIONO₂ results from an interaction of the oxygen atom of CIO with the nitrogen atom of the NO₂ where no entrance barrier is present, and it is stabilized by 29.8 kcal mol⁻¹. Furthermore, CIONO₂ can undergo a 1,3 migration of Cl and a rotation of O-Cl with energy barriers of 45.8 and 7.1 kcal mol⁻¹, respectively. CIONO₂ can break up into Cl and NO₃ radicals; this reaction step is found to be endothermic by 46.4 kcal mol⁻¹. The overall reaction NO₂ + OCl → NO₃ + Cl is endothermic by 16.6 kcal mol⁻¹. The CIOONO_{cp} and CIOONO_{ip} formation are exothermic by 5.4 and 3.8 kcal mol⁻¹, respectively, relative to CIO + NO₂. The inversion of the less stable CIOONO_{ip} to the CIOONO_{cp} minimum energy structure takes place by overcoming a 8.5 kcal mol⁻¹ energy barrier.

Finally, the different channels for isomerization of the CIOONO to CIONO₂ have been examined. The process should be exothermic by about 25 kcal mol⁻¹, but our present calculations show that it is unlikely due to the presence of high energy barriers for either possible isomerization pathways considered above. Even the activation barrier of 28.0 kcal mol⁻¹ predicted at the B3LYP/6-311G(d) level of theory for unimolecular isomerization is too high to account for appreciable nitrate formation from peroxyxynitrite.

ACKNOWLEDGMENT

This work was funded by the Ministry of Education, Science and Sport of Slovenia, grant number P2-0148 and partly by the NATO collaborative linkage grant EST.CLG.977083.

REFERENCES AND NOTES

- (1) Rowland, F. S.; Spencer, J. E.; Molina, M. J. Stratospheric Formation and Photolysis of Chlorine Nitrate. *J. Phys. Chem.* **1976**, *80*, 2711–2713.
- (2) Rowland, F. S.; Spencer, J. E.; Molina, M. J. Estimated Relative Abundance of Chlorine Nitrate among Stratospheric Chlorine Compounds. *J. Phys. Chem.* **1976**, *80*, 2713–2715.
- (3) Chang, J. S.; Barker, J. R.; Davenport, J. E.; Golden, D. M. Chlorine Nitrate Photolysis by a New Technique – Very Low-Pressure Photolysis. *Chem. Phys. Lett.* **1979**, *60*, 385–390.
- (4) Margitan, J. J. Chlorine Nitrate Photochemistry – Photolysis Products and Kinetics of the Reaction Cl + CIONO₂ → Cl₂ + NO₃. *J. Phys. Chem.* **1983**, *87*, 674–679.
- (5) Minton, T. K.; Nelson, C. M.; Moore, T. A.; Okumura, M. Direct Observation of CIO from Chlorine Nitrate Photolysis. *Science* **1992**, *258*, 1342–1345.
- (6) DeMore, W. B.; Sander, S. P.; Golden, D. M.; Hampson, R. F.; Kurylo, M. J.; Howard, C. J.; Ravishankara, A. R.; Kolb, C. E.; Molina, M. J. *JPL Publication 97-4*, **1997**, Evaluation 12.
- (7) Percival, C. J.; Smith, G. D.; Molina, L. T.; Molina, M. J. Temperature and Pressure Dependence of the Rate Constant for the CIO + NO₂ Reaction. *J. Phys. Chem. A* **1997**, *101*, 8830–8833.
- (8) Molina, M. J.; Molina, L. T.; Ishiwata, T. Kinetics of the CIO + NO₂ + M Reaction. *J. Phys. Chem.* **1980**, *84*, 3100–3104.
- (9) Bhatia, S. C.; Taylor, M. G.; Merideth, C. W.; Hall, J. H., Jr. Low-Temperature Infrared Spectrum of Chlorine Nitrate and Evidence for the Existence of CIOONO. *J. Phys. Chem.* **1983**, *87*, 1091–1093.
- (10) Griffith, D. W. T.; Tyndall, G. S.; Burrows, J. P.; Moortgat, G. K. Matrix-Isolation of Chlorine Nitrate. *Chem. Phys. Lett.* **1984**, *107*, 341–346.

- (11) McGrath, M. P.; Rowland, R. S. Determination of the Barriers to Internal Rotation in ONOOX (X=H, Cl) and Characterization of the Minimum Energy Conformers. *J. Phys. Chem.* **1994**, *98*, 1061–1067.
- (12) Bhatia, S. C.; Hall, J. H., Jr. Ab Initio Self-Consistent-Field Studies of ClNO_x (x=1–3). *J. Chem. Phys.* **1985**, *82*, 1991–1996.
- (13) McGrath, M. P.; Franci, M. M.; Rowland, R. S.; Hehre, W. J. Isomers of Nitric-Acid and Chlorine Nitrate. *J. Phys. Chem.* **1988**, *92*, 5352–5357.
- (14) Lamanna, G. An Ab Initio Study of the Molecular Structure of Chlorine Nitrate. *J. Mol. Struct. (THEOCHEM)* **1994**, *115*, 31–35.
- (15) Lee, T. J. A Coupled-Cluster Study of the Molecular Structure, Vibrational Spectrum, and Heats of Formation of XONO₂ (X=H, F, Cl). *J. Phys. Chem.* **1995**, *99*, 1943–1948.
- (16) Grana, A. M.; Lee, T. J.; Gordon, M. H. Ab Initio Calculations of Singlet and Triplet Excited States of Chlorine Nitrate and Nitric Acid. *J. Phys. Chem.* **1995**, *99*, 3493–3502.
- (17) Gaussian 98, Revision A.5, Frisch, M. J.; Trucks, G. W.; Schlegel, H. B.; Scuseria, G. E.; Robb, M. A.; Cheeseman, J. R.; Zakrzewski, V. G.; Montgomery, J. A., Jr.; Stratmann, R. E.; Burant, J. C.; Dapprich, S.; Millam, J. M.; Daniels, A. D.; Kudin, K. N.; Strain, M. C.; Farkas, O.; Tomasi, J.; Barone, V.; Cossi, M.; Cammi, R.; Mennucci, B.; Pomelli, C.; Adamo, C.; Clifford, S.; Ochterski, J.; Petersson, G. A.; Ayala, P. Y.; Cui, Q.; Morokuma, K.; Malick, D. K.; Rabuck, A. D.; Raghavachari, K.; Foresman, J. B.; Cioslowski, J.; Ortiz, J. V.; Stefanov, B. B.; Liu, G.; Liashenko, A.; Piskorz, P.; Komaromi, I.; Gomperts, R.; Martin, R. L.; Fox, D. J.; Keith, T.; Al-Laham, M. A.; Peng, C. Y.; Nanayakkara, A.; Gonzalez, C.; Challacombe, M.; Gill, P. M. W.; Johnson, B.; Chen, W.; Wong, M. W.; Andres, J. L.; Gonzalez, C.; Head-Gordon, M.; Replogle, E. S.; Pople, J. A. Gaussian, Inc., Pittsburgh, PA, 1998.
- (18) Hehre, W. J.; Radom, L.; Schleyer, P. v. R.; Pople, A. J. *Ab initio Molecular Orbital Theory*; Wiley-Interscience: New York, 1986; Chapter 2, pp 10–42.
- (19) Becke, A. D. Density Functional Thermochemistry. 3. The Role of Exact exchange. *J. Chem. Phys.* **1993**, *98*, 5648–5652.
- (20) Lee, C.; Yang, W.; Parr, R. G. Development of the Colle-Salvetti Correlation-Energy Formula into a Functional of the Electron Density. *Phys. Rev. B* **1988**, *37*, 785–789.
- (21) Miehlich, B.; Savin, A.; Stoll, H.; Preuss, H. Results Obtained with the Correlation Energy Density Functional of Becke and Lee, Yang and Parr. *Chem. Phys. Lett.* **1989**, *157*, 200–206.
- (22) Gonzales, C.; Schlegel, H. B. An Improved Algorithm for Reaction-Path Following. *J. Chem. Phys.* **1989**, *90*, 2154–2161.
- (23) Curtis, L. A.; Raghavachari, K.; Pople, J. A. Gaussian-2 theory using reduced Moller–Plesset orders. *J. Chem. Phys.* **1993**, *98*, 1293–1298.
- (24) Jacox, M. E. *J. Phys. Chem. Ref DATA* **1994**, Monograph No. 3.
- (25) Casper, B.; Lambotte, P.; Minkowitz, R.; Oberhammer, H. Gas-Phase Structures of Chlorine Nitrate and Bromine Nitrate (ClNO₂ and BrNO₂). *J. Phys. Chem.* **1993**, *97*, 9992–9995.
- (26) Lesar, A.; Prebil, S.; Mühlhäuser, M.; Hodošček, M. Conformational Potential Energy Surface of BrOONO. *Chem. Phys. Lett.* **2003**, *368*, 399–407.
- (27) Lesar, A.; Prebil, S.; Hodošček, M. Ab Initio Characterization of ClNO₃ Isomers. *J. Phys. Chem. A* **2003**, *107*, 9168–9174.
- (28) Tsai, H.-H.; Hamilton, T. P.; Tsai, J.-H. M.; Harrison, J. G.; Beckman, J. S. Comparison of ab Initio and Density Functional Theory for Alkali Peroxynitrite: A Highly Correlated System with Hartree–Fock Instability. *J. Phys. Chem.* **1996**, *100*, 6942.
- (29) Rohlfing, C. M. A Theoretical Study of HClO₃ Isomers. *Chem. Phys. Lett.* **1995**, *245*, 665–670.
- (30) Francisco, J. S.; Sander, S. P. Structures, Relative Stabilities, and Vibrational Spectra of Isomers of HClO₃. *J. Phys. Chem.* **1996**, *100*, 573–579.
- (31) Sumathi, R.; Peyerimhoff, S. D. Ab Initio Molecular Orbital Study of the Potential Energy Surface of the HO₂ + NO Reaction. *J. Chem. Phys.* **1997**, *107*, 1872–1880.
- (32) Lohr, L. L.; Barker, J. R.; Schroll, R. M. Modeling the Organic Nitrate Yields in the Reaction of Alkyl Peroxy Radicals with Nitric Oxide. 1. Electronic Structure Calculations and Thermochemistry. *J. Phys. Chem. A* **2003**, *107*, 7429–7433.
- (33) Lesar, A.; Hodošček, M. Transition State Structure and Energetics of the N₂O + X (X=Cl, Br) Reactions. *J. Chem. Inf. Comput. Sci.* **2002**, *42*, 706–711.

CI0497962